J. Coat. Technol. Res., **20** (2) 661–670, 2023
https://doi.org/10.1007/s11998-022-00699-7

Constructing robust and magnetic PU sponges modified with Fe_3O_4/GO nanohybrids for efficient oil/water separation

Dongdong Ge, Yun Zhang, Zhenshan Cui, Guilong Wang, Jun Liu, Xiaomeng Lv

Received: 27 March 2022 / Revised: 10 August 2022 / Accepted: 14 August 2022

Abstract Metal oxides, due to their low cost, environmental friendliness and wide sources, have attracted great attention. We chose iron oxide/graphene oxide (Fe_3O_4/GO) nanohybrids to modify a PU sponge to increase the surface roughness of the sponge without damaging its inherent structural properties. The composite was then treated with octadecane thiol to reduce the surface energy and produce a superhydrophobic and oleophilic absorption material with a water contact angle of 157°. From the absorption experiment with simulated oily water (including diesel oil, lubricating oil, rapeseed oil, chloroform, *N*,*N*-dimethyl formamide, tetrahydrofuran, ethanol and acetone), it was found that the Fe_3O_4/GO-modified PU sponge could absorb up to 80–170 times its own weight while showing outstanding recyclability achieved by squeeze/absorption cycles. Moreover, the composite absorption material exhibited weak magnetic properties, suggesting its recycling practicability. These results provide a quick and simple strategy to deal with oil spills and chemical leakage.

Keywords Graphene oxide, Fe_3O_4 nanoparticles, PU sponge, Superhydrophobic, Absorbent

Introduction

Superhydrophobic surfaces have received considerable attention from researchers because of their practical applications in diverse fields, such as self-cleaning,[1–6] anti-icing coatings,[6–10] anti-corrosion coatings,[10–14] oil–water separation,[15–19] corrosion resistance,[20] drag reduction,[21] and antifouling technologies.[22] In particular, in the oily water separation field, superhydrophobic materials play a significant role.[23] However, the traditional methods for separating oil from water usually show low separation efficiency and involve complex separation instruments, limiting their practical applications. Therefore, a desirable absorbent material with a high absorption capacity, good selectivity, excellent recyclability, a low cost and ease of operation is urgently needed.

Recently, metallic oxides have been applied in the superhydrophobic field because of their low cost, environmental friendliness and abundance. Many methods[24–27] for preparing superhydrophobic materials have been reported, such as the sol–gel process, chemical vapor deposition (CVD), layer-by-layer (LBL) assembly, and chemical etching. These methods are based on two key elements: (1) constructing a rough structure on a hydrophobic material surface and (2) coating low surface energy materials on a rough surface. To date, nanoparticles, especially metallic oxide nanoparticles such as TiO_2, ZnO, Al_2O_3, and Fe_3O_4, have been successfully coated on various substrates, showing an improvement in surface rough-

Supplementary Information The online version contains supplementary material available at https://doi.org/10.1007/s11998-022-00699-7.

D. Ge, Y. Zhang, G. Wang, J. Liu (✉)
School of the Environment and Safety Engineering, Jiangsu University, Zhenjiang 212013, People's Republic of China
e-mail: liujun1227@ujs.edu.cn

Z. Cui, X. Lv (✉)
School of Chemistry and Chemical Engineering, Jiangsu University, Zhenjiang 212013, People's Republic of China
e-mail: laiyangmeng@163.com

J. Liu
Suzhou University of Science and Technology, Suzhou 215009, People's Republic of China

X. Lv
Henan Province Key Laboratory of Water Pollution Control and Rehabilitation Technology, Pingdingshan 467036, People's Republic of China

ness.[28] El-Safty et al.[29] designed polydimethylsiloxane/graphene oxide nanosheets modified with hierarchical ZnO nanorods that exhibited superhydrophobic and anticorrosion performance. Li et al.[30] coated various metal oxide (ZnO, Al_2O_3, Fe_3O_4) nanoparticles on sponges, fabric and paper and then treated them with polydimethylsiloxane (PDMS) to obtain superhydrophobic surfaces. Mantilaka et al.[31] deposited ZnO on polyester fabric via electrodeposition, and the obtained fabric exhibited multifunctional properties, including superhydrophobic performance. Bismuth oxide was also considered to synergistically enhance superhydrophobic properties.[32] Among these substances, constructing a rough surface via the in situ growth of transition-metal oxides is important, and modification of the rough surface via the in situ growth of transition-metal/metal oxides is also crucial to achieve high superhydrophobicity. Thus, to ensure effective coating or to fix hydrophobic ingredients on a hydrophilic surface, the use of thiols as a surface modifying agent is currently becoming a prospective method.[33]

Herein, we successfully fabricated superhydrophobic and superoleophilic materials. First, we prepared iron oxide nanoparticles coated on the surface of a graphene oxide layer to obtain Fe_3O_4/GO nanohybrids. Then, the Fe_3O_4/GO nanohybrids were deposited on the surface of a PU sponge through the simple dipping method, and thiol groups were used as the surface modification to increase the number of hydrophobic -CH_3 functional groups. The rough surfaces and low surface energy rendered the composite material superhydrophobic. As a result, these hydrophobic properties endowed the modified PU sponge with potential applications in diverse organic solutions. Additionally, considering the flexibility of the PU sponge, the modified sponge possesses marvelous recyclability. Moreover, the prepared material has good prospects to combat oil spill pollution.

Experimental section

Preparation of Fe_3O_4/GO nanohybrids

In a typical synthesis, 40 mg of GO, 0.926 g of $FeSO_4{\cdot}7H_2O$ and 0.27 g of $FeCl_3$ were dispersed in 5 mL of HCl solution (0.01 mol L^{-1}) by sonication for 1 h. Then, the above mixture was added dropwise to 20 mL of $NH_3{\cdot}H_2O$ (3 mol L^{-1}) in a water bath for 4 h at 80°C. Finally, the Fe_3O_4/GO was removed, washed with deionized (DI) water until the pH reached 7, and dried in an oven for further use.

Synthesis of the M-PU sponge

The PU sponge was cut into blocks, ultrasonically treated with DI water and ethanol for 30 min each and dried in an oven at 60°C. The PU sponges were etched in a solution of chromium trichloride (100 g L^{-1}) and a sulfuric acid solution (98 wt.%) in turn for a few minutes each as pretreatment and then washed with DI water and dried in an oven. The PU sponge blocks were dipped into the Fe_3O_4/GO mixture solution and ultrasonicated every 6 h for 2–3 days. And finally, the sample was soaked in 50 mL 4 mmol L^{-1} alcohol solution of n-Octadecyl thiol for 30 min to obtain the modified polyurethane sponge adsorption material with superhydrophobic surface and labeled as the M-PU sponge.

Results and discussion

Processing of the PU sponge

PU sponges, well known for their porosity, large specific surface area, and ease of mass production, are good candidates for use as oil/water separation substrates. After the etching process, the PU sponge surface possesses many hydrophilic functional groups, such as -OH and -COOH, which bind the metal oxide particles in the PU sponge surface more easily. Additionally, the surface energy can be reduced by treatment with octadecane thiol, and the modified PU sponge can work as a superhydrophobic absorption material (Scheme 1).

Characterization of the Fe_3O_4/GO nanohybrids

As an effective and direct method, morphology observation can easily judge the adhesion effects of Fe_3O_4 nanoparticles on GO sheets. The resulting Fe_3O_4/GO nanohybrids were characterized by transmission electron microscopy (TEM) and scanning electron microscopy (SEM). The TEM images of the Fe_3O_4/GO nanohybrids are shown in Fig. 1a, 1b. It is clear that the iron oxide nanoparticles were distributed uniformly in the GO sheets, and the Fe_3O_4 nanoparticles were observed to have a uniform size of approximately 15 nm. SEM images of the materials indicated that their microstructure and morphology have quite conspicuous features. As shown in Fig. 1c, 1d, the Fe_3O_4 nanoparticles were densely distributed in the surface layer of GO. Increasing surface roughness helped to achieve the superhydrophobic feature.

The FTIR spectra of the Fe_3O_4/GO nanohybrids and graphene oxide are shown in Fig. 2a. GO displays a series of absorption bands ranging from 1050 to 3350 cm^{-1}, implying the presence of hydroxyl groups at 3350 cm^{-1}, carbonyl bonds from both ketone and carboxylic acid groups at 1730 cm^{-1}, aromatic C=C bonds and O–H bending vibrations at approximately 1620 cm^{-1}, C–OH stretching at 1360 cm^{-1}, C–O in alkoxy groups at 1050 cm^{-1}, and ether groups at 970 cm^{-1}. After coating the GO sheets with iron oxide

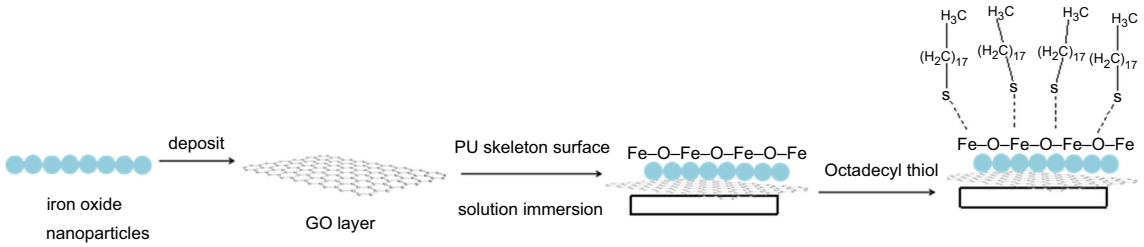

Scheme 1: Diagram of the experimental process

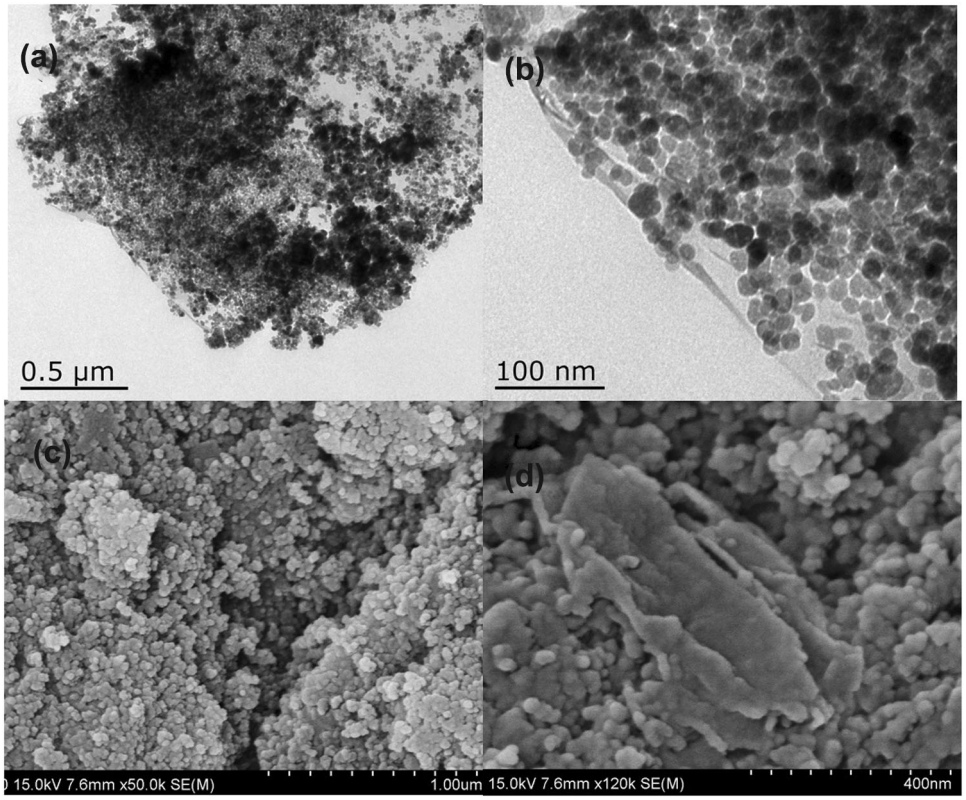

Fig. 1: TEM images of the Fe_3O_4/GO nanohybrids (a, b); SEM images of the Fe_3O_4/GO nanohybrids (c, d)

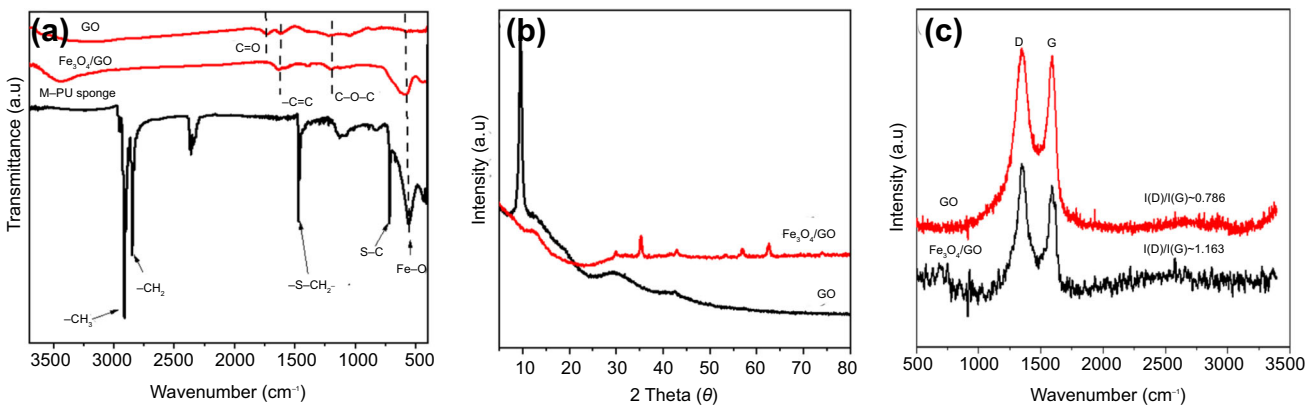

Fig. 2: FTIR spectra of GO, Fe_3O_4/GO and M-PU sponge (a), XRD patterns of GO and Fe_3O_4/GO (b), and Raman spectra of GO and the Fe_3O_4/GO nanohybrids

nanoparticles, the Fe_3O_4/GO nanohybrids showed the functional group Fe–O at 550 cm^{-1}. Moreover, compared to the GO curve, the disappearance of the peaks at approximately 1700 cm^{-1} is related to the C=O vibration of carboxylic groups, which indicates that these groups are involved in the reaction of unstable oxygen-containing groups. By observing the FTIR spectra of M-PU surface modified by octadecane thiol, it is found that the absorption peaks at 2920 and 2864 cm^{-1} are attributed to the stretching vibration absorption peaks of $–CH_3$ and $–CH_2$, respectively. At the same time, the plane wave vibration absorption peak of –S–C can be observed at 717 cm^{-1} and the deformation vibration absorption peak of $–S–CH_2$ can be observed at 1470 cm^{-1}, corresponding to a group with more than four $–CH_2$ in the carbon chains.[33] The characteristic absorption peak of C–O–C on the surface of M-PU sponge shifting towards smaller wavenumber, comparing with that of GO/Fe_3O_4 nanohybrids, indicates that a small amount of GO/Fe_3O_4 nanohybrids in the superhydrophobic coating is wrapped by n-octadecyl thiol, and octadecyl thiol was successfully modified on the sponge surface after the sponge was loaded with hybrid nanohybrids and then dipped in the ethanol dispersion of n-octadecyl thiol.

The XRD patterns of GO and Fe_3O_4/GO are displayed in Fig. 2b. GO exhibited a distinguished diffraction peak at 10.5°. The Fe_3O_4/GO nanohybrids exhibited five main characteristic diffraction peaks at 30°, 35°, 43°, 53°, 57° and 65°, which were assigned to the (220), (311), (400), (422), (511) and (440) lattices of the Fe_3O_4 nanohybrids (JCPDS no. 19-0629), respectively.[34] Correspondingly, the peak of GO was weakened after combination with iron oxide. Raman spectroscopy is one of the most convenient and effective methods to analyze and characterize carbon-based materials. For Raman spectra of GO (Fig. 2c), two intense peaks at 1300 and 1600 cm^{-1} were attributed to the D band corresponding to the defect sp^3 carbon structure and the G band corresponding to defect-free sp^2 hybridized atoms in carbon rings, respectively.[34–36] Regarding the Fe_3O_4/GO nanohybrids (Fig. 2c), the Raman peaks of the G and D bands shifted to lower frequencies compared with the spectrum displayed by pure GO. Moreover, the increased $I_{(D)}/I_{(G)}$ of the Fe_3O_4/GO nanohybrids was attributed to the introduction of Fe_3O_4 leading to more defects in the GO nanosheets.

Morphology and wettability of the M-PU sponge

The porous structure of the PU and M-PU sponges was observed by SEM, and the images are shown in Fig. 3. They have almost the same porous framework, which indicates that the Fe_3O_4/GO nanohybrids did not influence the hierarchical structure of the PU sponge. Compared to the smooth PU surface, the M-PU sponge skeleton is folded with a thin layer, as shown in Fig. 3c, which indicates that Fe_3O_4/GO nanocomposites are formed on the surface of the sponge. Additionally, it is clearly seen that the Fe_3O_4 nanoparticles are uniformly attached to the skeleton surface of the PU sponge.

To determine the hydrophobicity or oleophilicity of the M-PU sponge, its contact angle was measured. As shown in Fig. 4a, the water contact angle of the M-PU sponge reached 157°, which belongs to the superhydrophobic surface. In Fig. 4b, we can see that the M-PU sponge floats on the surface of water, while the PU sponge sinks after being placed under the water surface. All of the above facts confirmed that the M-PU sponge has stable superhydrophobicity.

To investigate the magnetic properties, a series of magnetic hysteresis curves of magnetic Fe_3O_4/GO nanohybrids and the M-PU sponges were recorded at room temperature, as shown in Fig. 5. The magnetic parameters of the samples at room temperature (including the saturation magnetization Ms, residual magnetization Mr and coercivity H) are as follows.

As shown in Table 1, the saturation magnetization (Ms), residual magnetization (Mr) and coercivity (H) of the Fe_3O_4/GO nanohybrids are 72.23 emu/g, 12.75 emu/g and 125.5 Oe, respectively. In inset of Fig. 5a, we can see that the Fe_3O_4/GO nanohybrids could separate from the water solution by their magnetic properties. Additionally, the Ms, Mr and H of the M-PU sponge were 1.51 emu/g, 0.23 emu/g, and 85.75 Oe due to the magnetic Fe_3O_4/GO nanohybrids uniformly dispersed on the surface of the PU sponge skeleton. Furthermore, the M-PU sponge has a certain weak magnetism (inset of Fig. 5b), which makes it more convenient and undergo a faster recovery during the recycling process.

Application of the M-PU sponge as an absorbent

The advantage of the M-PU sponge is that it is superhydrophobic and has a porous structure to absorb oil and nonpolar organic solvents without the suction of water, which renders it as an ideal and practical material for oil/water separation. The photographs in Fig. 6a show the fast and selective absorption of the M-PU sponge. When the M-PU sponge is in contact with the diesel oil layer (stained with Sudan III), it absorbs the diesel oil completely within 3 s. Moreover, we also tested the performance of high-density organic solvents (Fig. 6b), such as chloroform (stained with Sudan III). The results indicate that the M-PU sponge absorbs not only the low-density organic solvent but also the high-density organic solvent. Hence, the M-PU sponge is an ideal material for the removal of chemical leakage and oil spillage.

To further explore the absorption capacity of the M-PU sponge, we define the *Qe* value as the maximum absorbent value [Eq. (1), supporting information]. And before that, we first explored the adsorption capacity of untreated sponge and sponge containing nanohybrids without n-octadecyl thiol to chloroform with higher

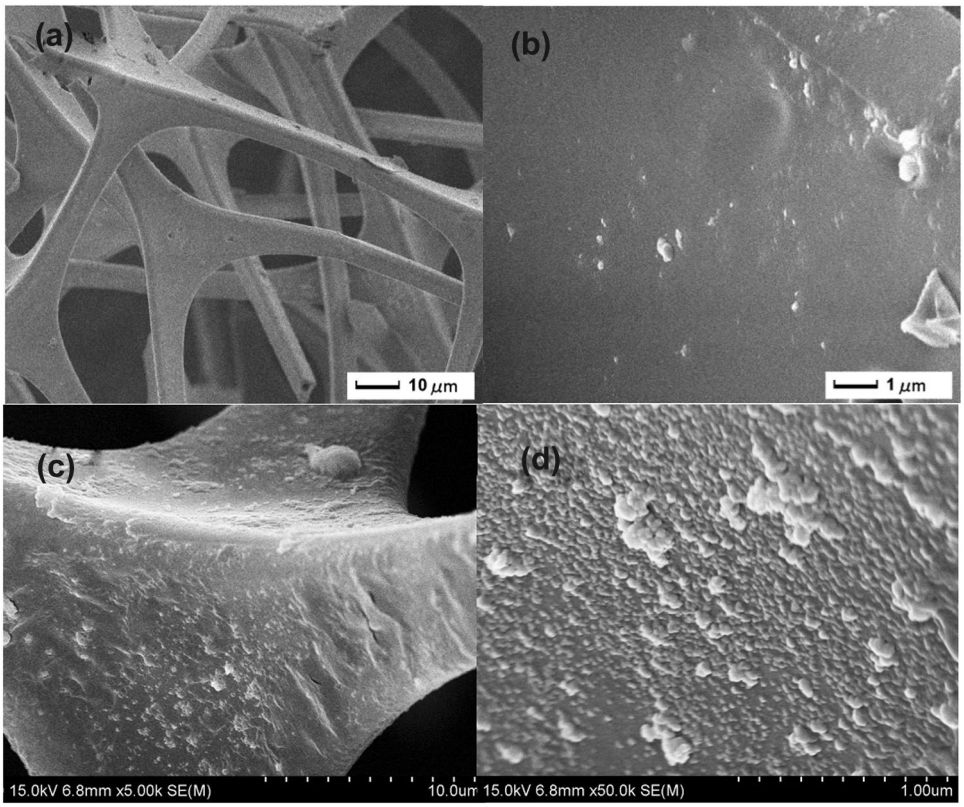

Fig. 3: SEM images of the PU sponge (a, b) and the M-PU sponge (c, d)

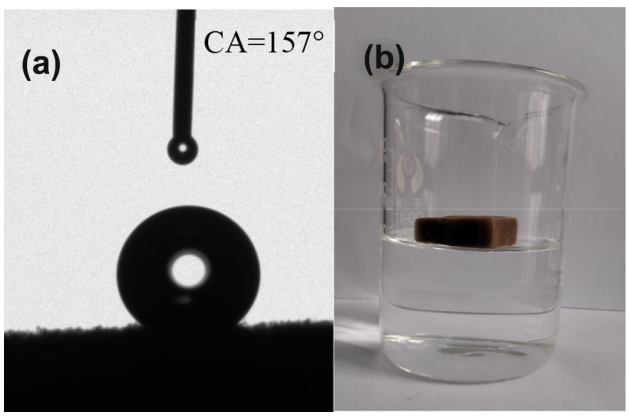

Fig. 4: Water contact angle of the M-PU sponge (a) and photo of the M-PU floating on the surface of water (b)

Table 1: The magnetism values of the Fe_3O_4/GO nanohybrids (a); M-PU sponge (b)

	Ms (emu/g)	Mr (emu/g)	Hc (Oe)
a	72.23	12.75	125.5
b	1.51	0.23	85.75

density, and the adsorption capacity was 40.70 times and 28.50 times of their own weight, respectively. Compared to the untreated sponge, the adsorption capacity of the sponge loaded with nanohybrids but without n-octadecyl thiol decreases because the surface of the sponge loaded with nanohybrids has a certain amount of hydrophilic hydroxyl groups, which leads to the weakening of the oleophilic of the sponge. Nevertheless, the M-PU sponge showed (Fig. 7a) its adsorption capacity ranges from approximately 80–170 times its own weight, depending on the density of solvents and oils, such as THF, ketones, DMF, hexane, benzyl alcohol, motor oil, diesel oil, rapeseed oil and chloroform. With the help of the thiol modification, the nanocomposite coating not only improves the roughness but also reduces the surface energy, thus improving its absorption performance. Compared to the absorption capacity of previously reported absorbents, the M-PU sponge shows much higher absorption abilities, for example, hierarchical micro-mesoporous carbon (< 1 time),[37] Fe_3O_4 nanoparticles (3.5 times),[38] cotton fiber-based sorbents (35.58 times),[39] conjugated microporous polymers (60–145 times),[40] magnetic hybrid gels (1–2 times),[41] cellulose nanofibril aerogels (28–47 times),[42] sponges based on polybenzoxazine and Fe_3O_4 (65.5–136.2 times),[43] chitosan–starch films (3–38 times),[44] vegetable fibers (85 times),[45] wood sponges with a spring-like lamellar structure (16–41 times),[46] chitin sponges (29–58 times),[47] and flexible

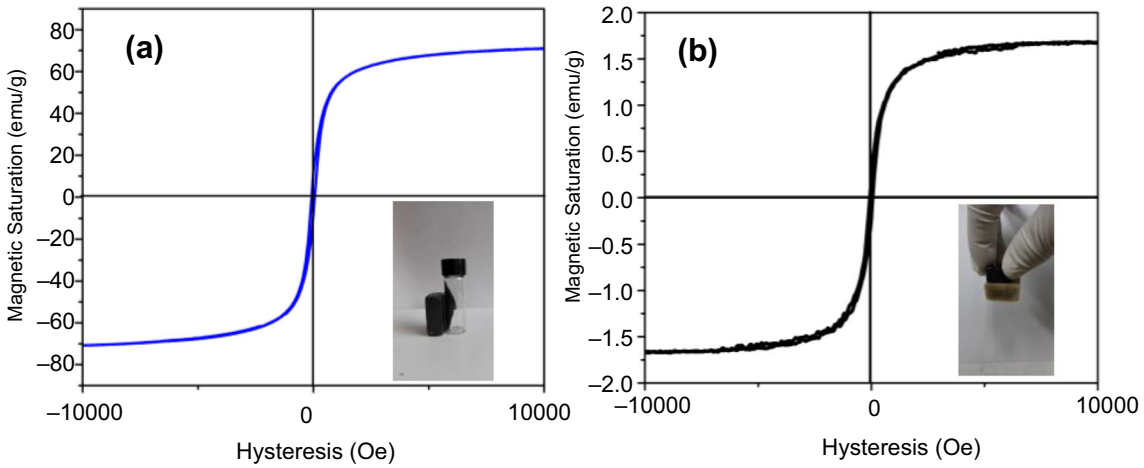

Fig. 5: Room temperature hysteresis curve of the Fe_3O_4/GO nanohybrids (a) and M-PU sponge (b)

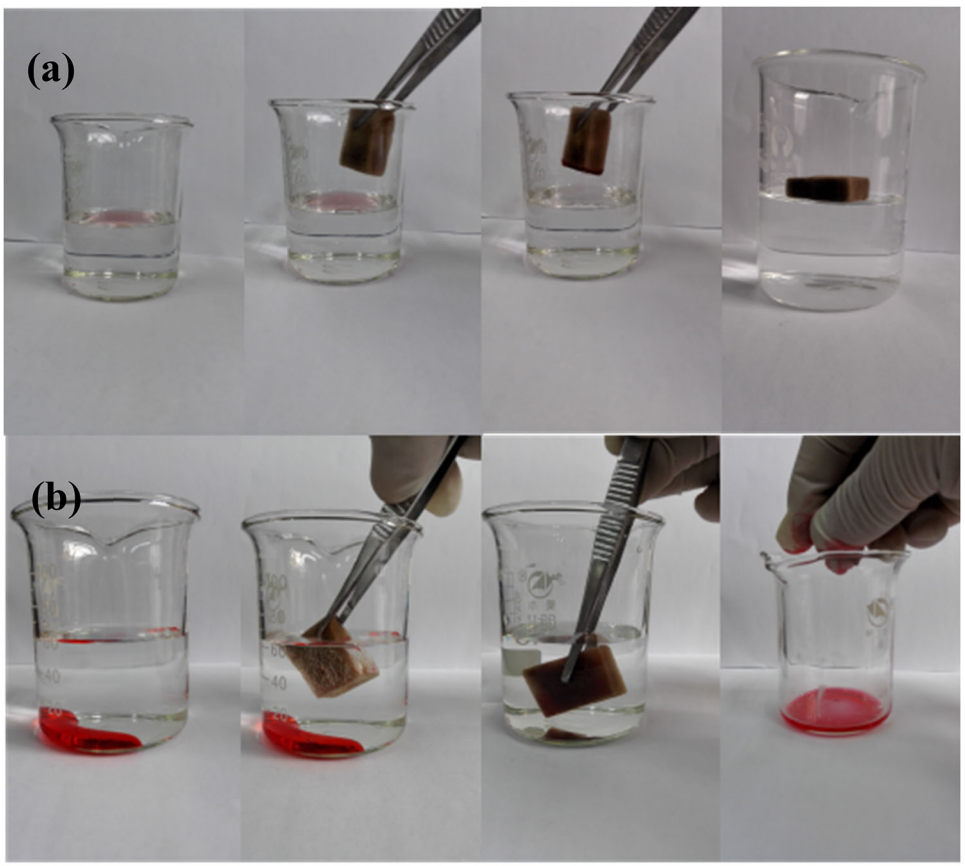

Fig. 6: Absorption of organic liquids by the M-PU sponge. The absorption process (from left to right) of diesel oil (stained with Sudan III) (a); the absorption process (from left to right) of chloroform (stained with Sudan III) (b)

silylated nanocellulose sponges (49–102 times),[48] Furthermore, the absorption capacity of the M-PU sponge is almost equal to that of materials with high absorption capacity, such as bubble-enhanced flexible bioaerogels (68–130 times),[49] nanocellulose aerogel foams (145–206 times),[50] cellulose aerogels (94–164 times),[51] and carbon microtube aerogels (78–348 times).[52] Furthermore, the absorption capacity of the M-PU sponge is still lower than that of other novel materials, for example, GCTs (250–400 times),[53] graphene foams (120–250 times),[54] nitrogen-doped graphene foam (200–600 times),[55] and ultra-flyweight aerogels (UFAs) (215–913 times).[56] Due to its excellent absorbency based on its remarkable surface

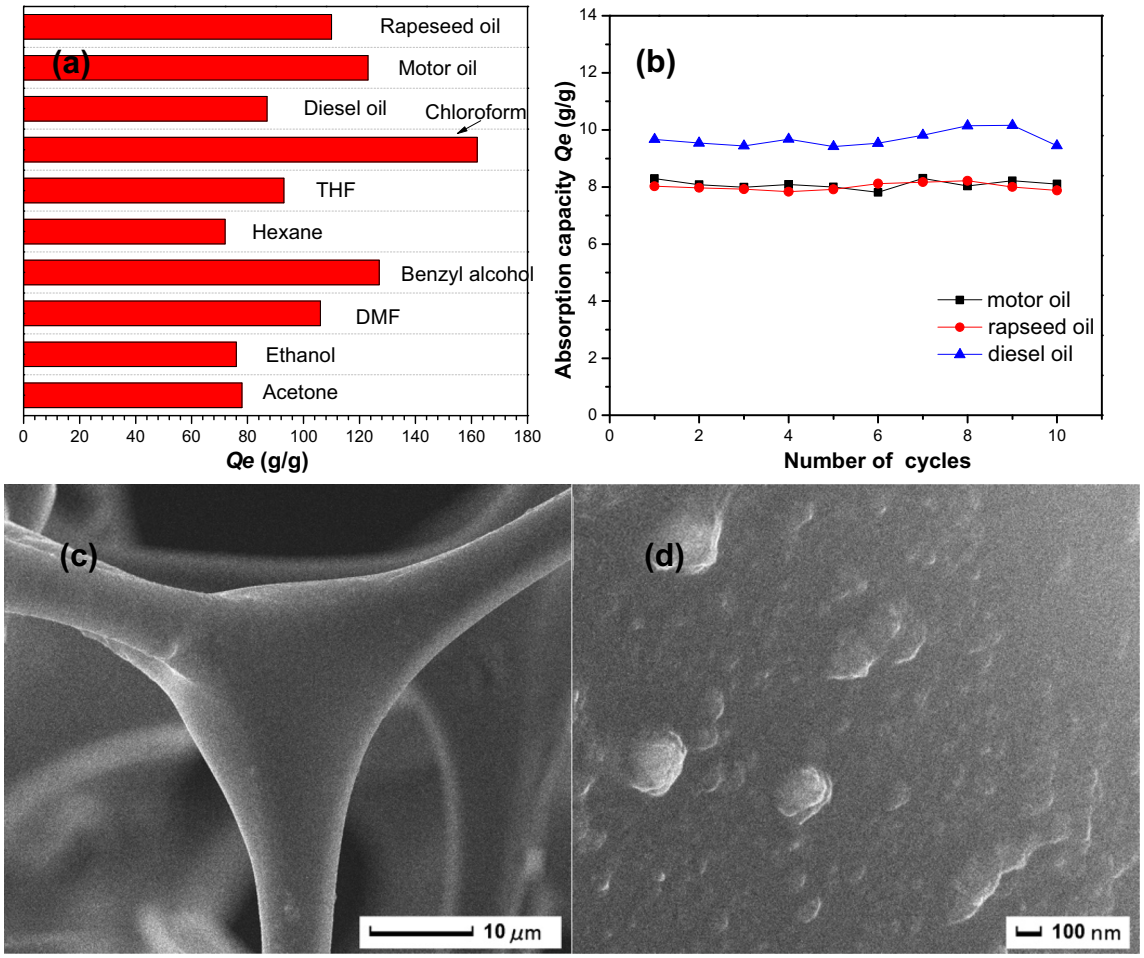

Fig. 7: The absorption capacity of the M-PU sponge over typical organic solvents and oil (a); absorption efficiency of the M-PU sponge on various organic liquids during the 10 cycles (b); SEM images of the M-PU sponge after 10 cycles (c, d)

superhydrophobic properties, the prepared M-PU sponges have exhibited potential applications, such as water treatment and oily water separation.

The cyclic absorption capacity is an important index to evaluate the superiority of adsorption materials. In this case, we adjusted the continuous mechanical squeezing method, which is vital for recycling. Therefore, we chose three common oils, motor oil, rapeseed oil and diesel oil, to evaluate the recycling ability of the M-PU sponges. In our former work,[57] we defined the value Qe' as the cycle absorption capacity of the M-PU sponge [Eq. (2), supporting information]. Figure 7b shows that the M-PU sponge could absorb up to 7–11 times its own weight of these oils after only 10 recycling processes. Furthermore, the absorption capacity itself did not significantly decrease, indicating that the M-PU sponge possesses stable absorption and recycling performance. The decrease in absorption capacity is mainly due to the calculated $\sim 10\%$ of the residual organic solvent on the M-PU sponge surface after each cycle. In addition, after 10 cycles, the microstructure of the M-PU sponge was observed, as shown in Fig. 7c, 7d. It can be clearly seen that the Fe_3O_4 nanoparticles are evenly distributed on the PU sponge surface, then, when the PU sponge surface is covered with a thin layer of oil, the graphene oxide fold lamellar structure is not obvious. Therefore, the M-PU sponge is a promising potential absorbent for the treatment of oily water separation.

Conclusions

In summary, we fabricated superhydrophobic, flexible and microporous M-PU sponges by coating PU sponge surfaces with Fe_3O_4/GO nanohybrids to form rough surfaces and treated them with octadecane thiol to reduce the surface energy. The absorption capacity of the M-PU sponge reached 170 times its own weight. More significantly, the M-PU sponge also possesses excellent cycling capacity after continuous mechanical squeezing methods. The magnetic properties of the M-PU sponge could make it more convenient with a faster recovery process. Due to the superior properties of the M-PU sponge, it would be an ideal potential absorbent for oily water separation.

Acknowledgments The research work is funded by the Zhenjiang Key Research and Development Program (GY2021004), the Opening Project of Henan Province Key Laboratory of Water Pollution Control and Rehabilitation Technology (CJSP2021006), Jiangsu Collaborative Innovation Center for Water Treatment Technology and Materials, and Innovation and Practice fund of Jiangsu University Industrial Center (ZXJG2021072).

Conflict of interest The authors have no competing interests to declare.

References

1. Wang, G, Li, A, Li, K, Zhao, Y, Ma, Y, He, Q, "A fluorine-free superhydrophobic silicone rubber surface has excellent self-cleaning and bouncing properties." *J. Colloid Interface Sci.*, **588** 175–183. https://doi.org/10.1016/j.jcis.2020.12.059 (2021)
2. Qing, Y, Long, C, An, K, Hu, C, Liu, C, "Sandpaper as template for a robust superhydrophobic surface with self-cleaning and anti-snow/icing performances." *J. Colloid Interface Sci.*, **548** 224–232. https://doi.org/10.1016/j.jcis.2019.04.040 (2019)
3. Fu, H, Liu, S, Yi, L, Jiang, H, Li, C, Chen, Y, "A durable and self-cleaning superhydrophobic surface prepared by precipitating flower-like crystals on a glass-ceramic surface." *Materials*, **13** (7) 1642. https://doi.org/10.3390/ma13071642 (2020)
4. Yang, T, Wang, M, Wang, X, Di, X, Wang, C, Li, Y, "Fabrication of a waterborne, superhydrophobic, self-cleaning, highly transparent and stable surface." *Soft Matter*, **16** (15) 3678–3685. https://doi.org/10.1039/C9SM02473E (2020)
5. Geyer, F, D'Acunzi, M, Sharifi-Aghili, A, Saal, A, Gao, N, Kaltbeitzel, A, Sloot, TF, Berger, R, Butt, HJ, Vollmer, D, "When and how self-cleaning of superhydrophobic surfaces works." *Sci. Adv.*, **6** eaaw272. https://doi.org/10.1126/sciadv.aaw9727 (2020)
6. Jiang, G, Chen, L, Zhang, S, Huang, H, "Superhydrophobic SiC/CNTs coatings with photothermal deicing and passive anti-icing properties." *ACS Appl. Mater. Interfaces*, **10** (42) 36505–36511. https://doi.org/10.1021/acsami.8b11201 (2018)
7. Han, Y, Liu, Z, Pan, W, Sun, J, "Electrochemically etched superhydrophobic surface on aeronautic steel with anti-icing, self-cleaning and durability property." *J. Phys: Conf. Ser.*, **2021** 012212. https://doi.org/10.1088/1742-6596/1948/1/012212 (1948)
8. Zhang, S, Huang, J, Cheng, Y, Yang, H, Chen, Z, Lai, Y, "Bioinspired surfaces with super wettability for anti-icing and Ice-phobic application: concept, mechanism, and design." *Small.*, **13** (48) 1701867. https://doi.org/10.1002/smll.201701867 (2017)
9. Li, Y, Li, B, Zhao, X, Tian, N, Zhang, J, "Totally waterborne, nonfluorinated, mechanically robust, and self-healing superhydrophobic coatings for actual anti-icing." *ACS Appl. Mater. Interfaces*, **10** (45) 39391–39399. https://doi.org/10.1021/acsami.8b15061 (2018)
10. Song, J, Li, Y, Xu, W, Liu, H, Lu, Y, "Inexpensive and non-fluorinated superhydrophobic concrete coating for anti-icing and anti-corrosion." *J. Colloid Interface Sci.*, **541** 86–92. https://doi.org/10.1016/j.jcis.2019.01.014 (2019)
11. Syed, JA, Tang, S, Meng, X, "Super-hydrophobic multilayer coatings with layer number tuned swapping in surface wettability and redox catalytic anti-corrosion application." *Sci. Rep.*, **7** (1) 4403. https://doi.org/10.1038/s41598-017-04651-3 (2017)
12. Yuan, J, Li, P, Yuan, R, Mao, D, "Fabrication and corrosion resistance of a superhydrophobic Ni-P/$Ni_3(NO_3)_2(OH)_4$ multilayer protective coating on magnesium alloy." *ACS Omega*, **5** (38) 24247–24255. https://doi.org/10.1021/acsomega.0c02196 (2020)
13. Chen, X, Wang, P, Zhang, D, "Designing a superhydrophobic surface for enhanced atmospheric corrosion resistance based on coalescence-induced droplet jumping behavior." *ACS Appl. Mater. Interfaces*, **11** (41) 38276–38284. https://doi.org/10.1021/acsami.9b11415 (2019)
14. Tong, W, Karthik, N, Li, J, Wang, N, Xiong, D, "Superhydrophobic surface with stepwise multilayered micro- and nanostructure and an investigation of its corrosion resistance." *Langmuir*, **35** (47) 15078–15085. https://doi.org/10.1021/acs.langmuir.9b02910 (2019)
15. Sam, EK, Liu, J, Lv, X, "Surface engineering materials of superhydrophobic sponges for oil/water separation: a review." *Ind. Eng. Chem. Res.*, **60** (6) 2353–2364. https://doi.org/10.1021/acs.iecr.0c05906 (2021)
16. Sam, EK, Ge, Y, Liu, J, Lv, X, "Robust, self-healing, superhydrophobic fabric for efficient oil/water emulsion separation." *Colloids Surf. A*, **625** 126860. https://doi.org/10.1016/j.colsurfa.2021.126860 (2021)
17. Kang, H, Zhao, B, Li, L, Zhang, J, "Durable superhydrophobic glass wool@polydopamine @PDMS for highly efficient oil/water separation." *J. Colloid Interface Sci.*, **544** 257–265. https://doi.org/10.1016/j.jcis.2019.02.096 (2019)
18. Du, B, Chen, F, Luo, R, Li, H, Zhou, S, Liu, S, Hu, J, "Superhydrophobic surfaces with pH-Induced switchable wettability for oil-water separation." *ACS Omega*, **4** (15) 16508–16516. https://doi.org/10.1021/acsomega.9b02150 (2019)
19. Zulfiqar, U, Thomas, AG, Matthews, A, Lewis, DJ, "Surface engineering of ceramic nanomaterials for separation of oil/water mixtures." *Front. Chem.*, **8** 578. https://doi.org/10.3389/fchem.2020.00578 (2020)
20. Liu, Y, Xue, J, Luo, D, Wang, H, Gong, X, Han, Z, Ren, L, "One-step fabrication of biomimetic superhydrophobic surface by electrodeposition on magnesium alloy and its corrosion inhibition." *J. Colloid Interface Sci.*, **491** 313–320. https://doi.org/10.1016/j.jcis.2016.12.022 (2017)
21. Tuo, Y, Zhang, H, Rong, W, Jiang, S, Chen, W, Liu, X, "Drag reduction of anisotropic superhydrophobic surfaces prepared by laser etching." *Langmuir*, **35** (34) 11016–11022. https://doi.org/10.1021/acs.langmuir.9b01040 (2019)
22. Xue, CH, Guo, XJ, Ma, JZ, Jia, ST, "Fabrication of robust and antifouling superhydrophobic surfaces via surface-initiated atom transfer radical polymerization." *ACS Appl. Mater. Interfaces*, **7** (15) 8251–8259. https://doi.org/10.1021/acsami.5b01426 (2015)
23. Abu-Thabit, NY, Uwaezuoke, OJ, Abu Elella, MH, "Superhydrophobic nanohybrid sponges for separation of oil/water mixtures." *Chemosphere*, **294** 133644. https://doi.org/10.1016/j.chemosphere.2022.133644 (2022)
24. Kwon, Y, Patankar, N, Choi, J, Lee, J, "Design of surface hierarchy for extreme hydrophobicity." *Langmuir*, **25** (11) 6129–6136. https://doi.org/10.1021/la803249t (2009)
25. Cha, SC, Her, EK, Ko, TJ, Kim, SJ, Roh, H, Lee, KR, Moon, MW, "Thermal stability of superhydrophobic, nanostruc-

tured surfaces.'' *J. Colloid Interface Sci.*, **391** 152–157. https://doi.org/10.1016/j.jcis.2012.09.052 (2013)
26. Shirtcliffe, NJ, McHale, G, Newton, MI, Perry, CC, ''Intrinsically superhydrophobic organosilica sol–gel foams.'' *Langmuir*, **19** 5626–5631. https://doi.org/10.1021/la034204f (2003)
27. Zhu, Y, Zhang, J, Zheng, Y, Huang, Z, Feng, L, Jiang, L, ''Stable, superhydrophobic, and conductive polyaniline/polystyrene films for corrosive environments.'' *Adv. Funct. Mater.*, **16** (4) 568–574. https://doi.org/10.1002/adfm.200500624 (2006)
28. Li, J, Shi, L, Chen, Y, Zhang, Y, Guo, Z, Su, B.-l, Liu, W, ''Stable superhydrophobic coatings from thiol-ligand nanocrystals and their application in oil/water separation.'' *J. Mater. Chem.*, **22** (19). https://doi.org/10.1039/c2jm30931a (2012)
29. Selim, MS, El-Safty, SA, Abbas, A, Shenashen, MA, ''Facile design of graphene oxide-ZnO nanorod-based ternary nanocomposite as a superhydrophobic and corrosion-barrier coating.'' *Colloids Surf. A*, **611** 1125793. https://doi.org/10.1016/j.colsurfa.2020.125793 (2021)
30. Bao, X-M, Cui, J-F, Sun, H-X, Liang, W-D, Zhu, Z-Q, An, J, Yang, P, La, PQ, Li, A, ''Facile preparation of superhydrophobic surfaces based on metal oxide nanoparticles.'' *Appl. Surf. Sci.*, **303** 473–480. https://doi.org/10.1016/j.apsusc.2014.03.029 (2014)
31. Ekanayake, UGM, Dayananda, KEDYT, Rathuwadu, N, Mantilaka, MMMGP, ''Fabrication of multifunctional smart polyester fabric via electrochemical deposition of ZnO nano-/microhierarchical structures.'' *J. Coat. Technol. Res.* https://doi.org/10.1007/s11998-021-00606-6 (2022)
32. Zong, L, Wu, Y, Jiang, B, ''The preparation of superhydrophobic photocatalytic fluorosilicone/SiO_2–TiO_2 coating and its self-cleaning performance.'' *J. Coat. Technol. Res.*, **18** 1245–1259. https://doi.org/10.1007/s11998-021-00485-x (2021)
33. Yang, X, Yang, N, Gong, Z, Peng, F, Jiang, B, Sun, Y, Zhang, L, ''The superhydrophobic sponge decorated with Ni–Co double layered oxides with thiol modification for continuous oil/water separation.'' *Chin. J. Chem. Eng.*. https://doi.org/10.1016/j.cjche.2022.03.023 (2022)
34. Liu, M, Wen, T, Wu, X, Chen, C, Hu, J, Li, J, Wang, X, ''Synthesis of porous Fe_3O_4 hollow microspheres/graphene oxide composite for Cr (VI) removal.'' *Dalton Trans.*, **42** (41) 14710–14717. https://doi.org/10.1039/c3dt50955a (2013)
35. Sui, D, Wu, M, Liu, Y, Yang, Y, Zhang, H, Ma, Y, Chen, Y, ''High performance Li-ion capacitor fabricated with dual graphene-based materials.'' *Nanotechnology*, **32** (1) 015403. https://doi.org/10.1088/1361-6528/abb9d8 (2021)
36. Sui, D, Xu, L, Zhang, H, Sun, Z, Kan, B, Ma, Y, Chen, Y, ''A 3D cross-linked graphene-based honeycomb carbon composite with excellent confinement effect of organic cathode material for lithium-ion batteries.'' *Carbon*, **157** 656–662. https://doi.org/10.1016/j.carbon.2019.10.106 (2020)
37. An, Z, Kong, S, Zhang, W, Yuan, M, An, Z, Chen, D, ''Synthesis and adsorption performance of a hierarchical micro-mesoporous carbon for toluene removal under ambient conditions.'' *Materials*, **13** (3) 13894–13901. https://doi.org/10.3390/ma13030716 (2020)
38. Rozi, SKM, Shahabuddin, S, Manan, NSA, Mohamad, S, Kamal, SAA, Rahman, SA, ''Palm fatty acid functionalized Fe_3O_4 nanoparticles as highly selective oil adsorption material.'' *J. Nanosci. Nanotechnol.*, **18** (5) 3248–3256. https://doi.org/10.1166/jnn.2018.14699 (2018)
39. Shin, Y, Han, KS, Arey, BW, Bonheyo, GT, ''Cotton fiber-based sorbents for treating crude oil spills.'' *ACS Omega*, **5** (23) 13894–13901. https://doi.org/10.1021/acsomega.0c01290 (2020)
40. Xiao, Z, Zhang, M, Fan, W, Qian, Y, Yang, Z, Xu, B, Kang, Z, Wang, R, Sun, D, ''Highly efficient oil/water separation and trace organic contaminants removal based on superhydrophobic conjugated microporous polymer coated devices.'' *Chem. Eng. J.*, **326** 640–646. https://doi.org/10.1016/j.cej.2017.06.023 (2017)
41. Scheverin, N, Fossati, A, Horst, F, Lassalle, V, Jacobo, S, ''Magnetic hybrid gels for emulsified oil adsorption: an overview of their potential to solve environmental problems associated to petroleum spills.'' *Environ. Sci. Pollut. Res. Int.*, **27** (1) 861–872. https://doi.org/10.1007/s11356-019-06752-0 (2020)
42. Korhonen, JT, Kettunen, M, Ras, RH, Ikkala, O, ''Hydrophobic nanocellulose aerogels as floating, sustainable, reusable, and recyclable oil absorbents.'' *ACS Appl. Mater. Interfaces*, **3** (6) 1813–1816. https://doi.org/10.1021/am200475b (2011)
43. Zhu, Y, Du, Y, Su, J, Mo, Y, Yu, S, Wang, Z, ''Durable superhydrophobic melamine sponge based on polybenzoxazine and Fe_3O_4 for oil/water separation.'' *Sep. Purif. Technol.*, **275** 119130. https://doi.org/10.1016/j.seppur.2021.119130 (2021)
44. Lozano-Navarro, JI, Díaz-Zavala, NP, Melo-Banda, JA, Velasco-Santos, C, Paraguay-Delgado, F, Peréz-Sánchez, JF, Domínguez-Esquivel, JM, Suárez-Domínguez, EJ, Sosa-Sevilla, JE, ''Chitosan–starch films modified with natural extracts to remove heavy oil from water.'' *Water*, **12** (1) 17. https://doi.org/10.3390/w12010017 (2019)
45. Annunciado, TR, Sydenstricker, T, Amico, SC, ''Experimental investigation of various vegetable fibers as sorbent materials for oil spills.'' *Mar Pollut Bull.*, **50** (11) 1340–1346. https://doi.org/10.1016/j.marpolbul.2005.04.043 (2005)
46. Guan, H, Cheng, Z, Wang, X, ''Highly compressible wood sponges with a spring-like lamellar structure as effective and reusable oil absorbents.'' *ACS Nano.*, **12** (10) 10365–10373. https://doi.org/10.1021/acsnano.8b05763 (2018)
47. Duan, B, Gao, H, He, M, Zhang, L, ''Hydrophobic modification on surface of chitin sponges for highly effective separation of oil.'' *ACS Appl. Mater. Interfaces*, **6** (22) 19933–19942. https://doi.org/10.1021/am505414y (2014)
48. Zhang, Z, Sèbe, G, Rentsch, D, Zimmermann, T, Tingaut, P, ''Ultralightweight and flexible silylated nanocellulose sponges for the selective removal of oil from water.'' *Chem. Mater.*, **26** (8) 2659–2668. https://doi.org/10.1021/cm5004164 (2014)
49. Wang, Q, Qin, Y, Xue, C, Yu, H, Li, Y, ''Facile fabrication of bubbles-enhanced flexible bioaerogels for efficient and recyclable oil adsorption.'' *Chem. Eng. J.*, **402** 126240. https://doi.org/10.1016/j.cej.2020.126240 (2020)
50. Zhang, H, Lyu, S, Zhou, X, Gu, H, Ma, C, Wang, C, Ding, T, Shao, Q, Liu, H, Guo, Z, ''Super light 3D hierarchical nanocellulose aerogel foam with superior oil adsorption.'' *J. Colloid Interface Sci.*, **536** 245–251. https://doi.org/10.1016/j.jcis.2018.10.038 (2019)
51. Li, Z, Zhong, L, Zhang, T, Qiu, F, Yue, X, Yang, D, ''Sustainable, flexible, and superhydrophobic functionalized cellulose aerogel for selective and versatile oil/water separation.'' *ACS Sustain. Chem. Eng.*, **7** (11) 9984–9994. https://doi.org/10.1021/acssuschemeng.9b01122 (2019)
52. Song, P, Cui, J, Di, J, Liu, D, Xu, M, Tang, B, Zeng, Q, Xiong, J, Wang, C, He, Q, Kang, L, Zhou, J, Duan, R, Chen, B, Guo, S, Liu, F, Shen, J, Liu, Z, ''Carbon microtube aerogel derived from kapok fiber: An efficient and recyclable sorbent for oils and organic solvents.'' *ACS Nano*, **14** (1) 595–602. https://doi.org/10.1021/acsnano.9b07063 (2020)

53. Shi, L, Chen, K, Du, R, Bachmatiuk, A, Ruemmeli, MH, Xie, K, Huang, Y, Zhang, Y, Liu, Z, ''Scalable seashell-based chemical vapor deposition growth of three-dimensional graphene foams for oil-water separation.'' *J. Am. Chem. Soc.*, **138** (20) 6360. https://doi.org/10.1021/jacs.6b02262 (2016)
54. Chen, J, Shen, X, Pan, Y, Liu, C, Hwang, SY, Xu, Q, Peng, Z, ''Synthesis of freestanding amorphous giant carbon tubes with outstanding oil sorption and water oxidation properties.'' *J. Mater. Chem. A*, **6** (9) 3996–4002. https://doi.org/10.1039/c7ta09822g (2018)
55. Lü, X, Cui, Z, Wei, W, Xie, J, Jiang, L, Huang, J, Liu, J, ''Constructing PU sponge modified with silica/graphene oxide nanohybrids as a ternary sorbent.'' *Chem Eng. J.*, **284** 478–486. https://doi.org/10.1016/j.cej.2015.09.002 (2016)
56. Sun, H, Xu, Z, Gao, C, ''Multifunctional, ultra-flyweight, synergistically assembled carbon aerogels.'' *Adv. Mater.*, **25** (18) 2554–2560. https://doi.org/10.1002/adma.201204576 (2013)
57. Zhao, Y, Hu, C, Hu, Y, Cheng, H, Shi, G, Qu, L, ''A versatile, ultralight, nitrogen-doped graphene framework.'' *Angew. Chem. Int. Ed.*, **124** 11533–11537. https://doi.org/10.1002/ange.201206554 (2012)